Articles

Synthesis and Excited State Raman Spectroscopy of Sterically Crowded Ruthenium(II) Octaethyltetraphenylporphyrin

S. E. Vitols,† J. Scott Roman, Daniel E. Ryan,‡ Milton E. Blackwood, Jr., and Thomas G. Spiro*

Department of Chemistry, Princeton University, Princeton, New Jersey 08544-1009

Received June 27, 1996[⊗]

Pyridine and CO adducts of Ru^{II}OETPP (OETPP = 2,3,7,8,12,13,17,18-octaethyl-5,10,15,20-tetraphenylporphinato) have been prepared and characterized by absorption and resonance Raman (RR) spectroscopy. Ru → porphyrin back-bonding is evident from the ground state RR spectra. Skeletal mode frequency downshifts in Ru^{II}OETPP-$(Py)_2$ relative to Ru^{II}OETPP(CO)(Py) are comparable to those seen for the TPP (tetraphenylporphyrin) and OEP (octaethylporphyrin) analogs, indicating that distortion of the porphyrin ring from substituent crowding has little effect on the extent of back-bonding. Photoexcited Ru^{II}OETPP$(Py)_2$ has absorption and RR spectra which are similar to those of Ru^{II}TPP$(Py)_2$ and are characteristic of a ($d\pi,\pi^*$) charge transfer state. As for Ru^{II}TPP$(Py)_2$, the photoexcited RR spectrum has features indicating porphyrin anion formation and does not have pyridine anion features, as have been observed for photoexcited Ru^{II}OEP$(Py)_2$. The ethyl substituents raise the porphyrin e_g* orbital above the lowest pyridine π* orbital in Ru^{II}OEP$(Py)_2$, but not in Ru^{II}OETPP$(Py)_2$, for which the effect of the phenyl substituents is dominant.

Introduction

The highly distorted dodecasubstituted porphyrins have attracted much interest[1−3] as model systems for studying the effects of nonplanar conformational distortions on the biological properties of the tetrapyrroles found in the photosynthetic reaction center of *Rhodopseudomanas viridis*[4,5] and the antenna system of *Prosthecochloris viridis*.[6] In the models, steric crowding of the peripheral substituents takes the place of environmental influences from the surrounding protein in the photosynthetic systems[7] and permits systematic exploration of the electronic effects of out-of-plane distortions.

The steric clash of substituents at the *meso* and pyrrole β positions (Figure 1) can produce ruffled or saddle-shaped porphyrins.[1,2] The lowered symmetry increases the complexity of the vibrational spectrum by splitting degeneracies and destroying the mutual exclusion of Raman and infrared modes.[3,8,9] Optical properties are also affected. Relative to TPP and OEP complexes, the Soret and Q bands of OETPP's are red-shifted, reflecting destabilization of the highest occupied molecular orbital.[1c] The fluorescence spectrum is also red-shifted and exhibits an anomalously large absorption/fluorescence Stokes

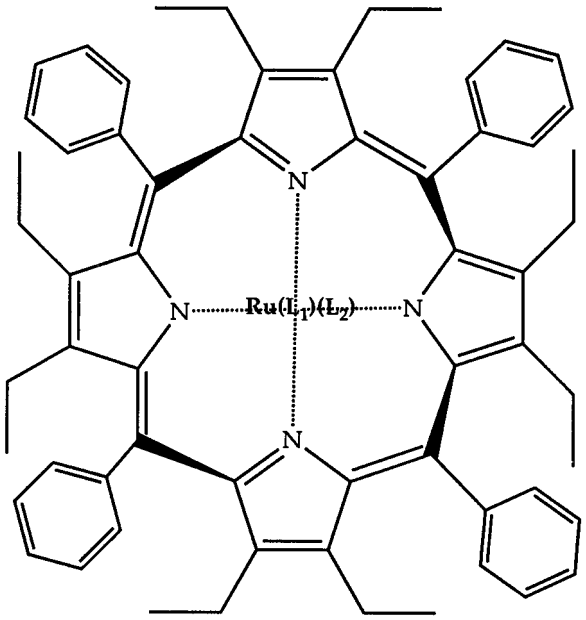

Figure 1. Structural diagram for Ru^{II}OETPP.

* To whom correspondence should be addressed.
† Present address: CST-4 MS J586 TA-46, Spectroscopy and Biophysics Group, Los Alamos National Laboratory, Los Alamos, NM 87545.
‡ Present address: Department of Biology, California Institute of Technology, Pasadena, CA 91125.
⊗ Abstract published in *Advance ACS Abstracts,* February 1, 1997.

(1) (a) Barkigia, K. M.; Berber, M. D.; Fajer, J.; Medforth, C. J.; Renner, M. W.; Smith, K. M. *J. Am. Chem. Soc.* **1990**, *112*, 8851. (b) Senge, M. O.; Medforth, C. J.; Sparks, L. D.; Shelnutt, J. A.; Smith, K. M. *Inorg. Chem.* **1993**, *32*, 1716. (c) Barkigia, K. M.; Renner, M. W.; Furenlid, L. R.; Medforth, C. J.; Smith, K. M.; Fajer, J. *J. Am. Chem. Soc.* **1993**, *115*, 3627. (d) Jentzen, W.; Simpson, M. C.; Hobbs, J. D.; Song, X.; Ema, T.; Nelson, N. Y.; Medforth, C. J.; Smith, K. M.; Veyrat, M.; Mazzanti, M.; Ramasseul, R.; Marchon, J.-C.; Takeuchi, T.; Goddard, W. A., III; Shelnutt, J. A. *J. Am. Chem. Soc.* **1995**, *117*, 11085−11097.
(2) Medforth, C. J.; Senge, M. O.; Smith, K. M.; Shelnutt, J. A. *J. Am. Chem. Soc.* **1992**, *114*, 9859.
(3) Piffat, C.; Melamed, D.; Spiro, T. G. *J. Phys. Chem.* **1993**, *97*, 7441.
(4) Deisenhofer, J.; Michel, H. *Science* **1989**, *245*, 1463.
(5) Horning, T. L.; Fujita, E.; Fajer, J. *J. Am. Chem. Soc.* **1986**, *108*, 323.
(6) Tronrud, D. E.; Schmid, M. F.; Matthews, B. W. *J. Mol. Biol.* **1986**, *188*, 443.
(7) Barkigia, K. M.; Chantranupong, L.; Smith, K. M.; Fajer, J. *J. Am. Chem. Soc.* **1988**, *110*, 7566.
(8) Shelnutt, J. A.; Majumder, S. A.; Sparks, L. D.; Hobbs, J. D.; Medforth, C. J.; Senge, M. O.; Smith, K. M.; Miura, M.; Luo, L.; Quirke, J. M. E. *J. Raman Spectrosc.* **1992**, *23*, 525.
(9) Sparks, L. D.; Medforth, C. J.; Park, M.-S.; Chamberlain, J. R.; Ondrias, M. R.; Senge, M. O.; Smith, K. M.; Shelnutt, J. A. *J. Am. Chem. Soc.* **1993**, *115*, 581.

S0020-1669(96)00773-2 CCC: $14.00

shift, as well as reduced quantum yield.[10−12] Recent time-resolved emission and picosecond transient absorption studies[13] indicate that increased rates of both intersystem crossing (S_1/T_1) and internal conversion (S_1/S_0) account for the reduced quantum yield; a large structural reorganization in the $^1(\pi,\pi^*)$ excited state may account for the large Stokes shift.[13]

Possible implications of the distortions for the mechanism of photoinduced electron transfer have been addressed.[7] However, to date, no distorted dodecasubstituted porphyrin has been made which produces a charge-separated state upon photoexcitation. To explore this dimension, we have prepared Ru(II) adducts of OETPP (Figure 1), since ruthenium porphyrins form photoinduced metal-to-ligand charge transfer states (MLCT)[14−16] when the Ru(II) d orbital energies are tuned by appropriate choice of axial ligand. The MLCT state is the lowest lying excited state when pyridine is the axial ligand, but it is raised above the $^3\pi-\pi^*$ state when the axial ligand is CO, which lowers the d_π orbital energy via back-bonding. It is of interest to discover whether out-of-plane distortion of the porphyrin affects the excited state ordering by perturbing the orbital energies. In addition, the nature of the MLCT state is at issue. Transient RR spectroscopy has established that the character of the state depends on the porphyrin substituents.[16] In $Ru^{II}TPP(Py)_2$ the acceptor orbital is a porphyrin π^* orbital, but in $Ru^{II}OEP(Py)_2$ the acceptor orbital is, surprisingly, on the axial pyridine ligands. It is therefore of considerable interest to find out where the electron goes when the porphyrin contains both phenyl and ethyl substituents.

Experimental Section

General Information. Visible and FTIR spectra were obtained on Hewlett-Packard 8452A and Nicolet 5DXB spectrometers, repectively. ^{1}H NMR spectra were taken on a JEOL GSX-270 (270 MHz) spectrometer. Chemical shifts are reported in ppm relative to residual solvent resonance (δ 7.24 for $CHCl_3$). FAB-MS analyses were performed on a Kratos MS5ORFTC mass spectrometer, and 3-nitrobenzyl alcohol was used to form the sample matrix.

Materials. Methylene chloride was distilled over calcium hydride and passed through a basic alumina column immediately prior to use. Benzene and diethyl ether were distilled over sodium/benzophenone. Tetrahydrofuran was passed through basic alumina and then distilled from sodium/benzophenone. Dimethyl sulfoxide was freshly distilled and stored over molecular sieves (4 Å). Propionaldehyde and benzaldehyde were freshly distilled before use. Deuteriochloroform was stored over K_2CO_3/molecular sieves and passed through a basic alumina column before use. $Ru_3(CO)_{12}$ was purified by dissolution in benzene, filtration, and removal of solvent under reduced pressure. All other reagents were obtained from Aldrich and used without further purification.

3-Hexen-2-one. The synthesis followed established procedures,[17,18] with slight modifications. To an argon-purged solution of 1-(triphenylphosphoranylidene)-2-propanone (25.00 g, 78.5 mmol) in 100 mL of CH_2Cl_2 was added 6.25 mL (86.6 mmol) of propionaldehyde via syringe. After 72.5 h of stirring at room temperature, the yellow reaction mixture was concentrated under reduced pressure and the resulting white solid triphenylphosphine oxide was filtered off onto a glass frit and washed with *n*-pentane. Most of pentane was removed by vacuum distillation with a water aspirator. The product distilled as a clear liquid at 129−130 °C to yield 5.593 g (72.6%) of 3-hexen-2-one. ^{1}H NMR ($CDCl_3$): δ 6.79 (dt, 1H, J = 6.1 Hz, H at C-4), 6.00 (dt, 1H, J = 1.3 Hz, 16.1 Hz, H at C-3), 2.22−2.16 (m, 2H, H at C-5), 2.18 (s, 3H, H at C-1), 1.02 (t, 3H, J = 7.4 Hz, H at C-6). NMR of the isolated $Ph_3P{=}O$ (21.6 g, 98.9%) in $CDCl_3$ was identical to that of a reference sample.

3-Acetyl-4-ethylpyrrole. According to the literature procedure,[19] in a dry flask under argon, 1.34 g of NaH (60% dispersion in mineral oil, 33.6 mmol) was rinsed with hexane (3 × 7.5 mL), added via syringe and removed via cannula. Diethyl ether (30 mL) was then syringed into the flask. A solution of 3-hexen-2-one (1.50 g, 15.3 mmol) and (*p*-tolylsulfonyl)methyl isocyanide (TOSMIC) (2.98 g, 15.3 mmol) in 90 mL of 2:1 ether/DMSO was prepared in another flask under argon and was slowly added via cannula to the NaH slurry over a period of 50 min. Evolution of gas and formation of a tan solid were observed during the addition. After another 40 min of stirring at room temperature, the mixture was cooled in an ice bath and the reaction slowly quenched with 60 mL of of H_2O. The aqueous layer was removed and extracted with ether (4 × 30 mL). The combined ether extracts were washed with aqueous NaCl and dried over Na_2SO_4. After removal of solvent, the residue was taken up in CH_2Cl_2 and and the solution chromatographed on neutral alumina (activity I, CH_2Cl_2) to yield a pale yellow oil which solidified upon cooling to −15 °C (1.73 g, 82.4%). ^{1}H NMR ($CDCl_3$): δ 8.98 (s (br), 1H, NH), 7.36 (t, 1H, J = 2.4 Hz, H at C-5), 6.56 (s (br), 1H, H at C-2), 2.78 (q, 2H, J = 7.4 Hz, CH_2), 2.38 (s, 3H, $COCH_3$), 1.17 (t, 3H, J = 7.4 Hz, CH_2CH_3).

3,4-Diethylpyrrole. According to established procedures,[17,20] to a stirred mixture of lithium aluminum hydride (LAH) (2.67 g, 70.4 mmol) in 75 mL of THF under argon at 25 °C was added a solution of 3-acetyl-4-ethylpyrrole (1.73 g, 12.6 mmol) in 50 mL of THF via cannula over a period of 2.5 h. The reaction mixture became a pale lime green color and was allowed to stir for an additional 21.5 h at room temperature, at which point it was heated to relux for 2 h. The solution was then cooled to 0 °C and the reaction quenched by the sequential dropwise addition of 2.7 mL of H_2O, 2.7 mL of 15% aqueous NaOH, and 8.1 mL of H_2O. Stirring was continued at 0 °C for 30 min, anhydrous $MgSO_4$ was then added, and stirring was resumed at room temperature for another 30 min. The solid was removed by suction filtration and washed with THF. The pale yellow filtrate was concentrated under reduced pressure to ∼15 mL and then diluted with 50 mL of ether and 50 mL of saturated aqueous NaCl. The aqueous layer was extracted with ether (3 × 50 mL), and the combined extracts were washed with aqueous NaCl and dried over Na_2SO_4. Removal of solvent and brief vacuum-drying yielded a viscous yellow oil which solidified upon cooling to −15 °C (1.34 g, 86.5%). ^{1}H NMR ($CDCl_3$): δ 7.82 (s (br), 1H, NH), 6.52 (d, 2H, J = 2.6 Hz, H at C-2 and C-5), 2.45 (q, 4H, J = 7.6 Hz, CH_2), 1.19 (t, 6H, J = 7.6 Hz, CH_3).

2,3,7,8,12,13,17,18-Octaethyl-5,10,15,20-tetraphenylporphyrin [OETPP(H_2)]. According to the referenced procedure with some modification,[1a] a 2 L, two-necked flask was charged with 1 L of distilled CH_2Cl_2, 3,4-diethylpyrrole (1.34 g, 10.9 mmol), and benzaldehyde (1.10 mL, 10.8 mmol). The flask was equipped with a reflux condenser and was purged with argon for 15 min. The reaction vessel was then sealed with a septum, and $BF_3{\cdot}OEt_2$ (0.134 mL, 1.09 mmol) was added via syringe. The reaction mixture was shielded from ambient light and was stirred continuously for 75 min at room temperature. The pale orange solution was then concentrated under reduced pressure to a dark purple, oily residue, which was dissolved in 75 mL of methanol and stored overnight at −10 °C. The methanol solution was filtered onto a glass frit, and the solid was washed with excess MeOH until the filtrate was practically clear. The mauve solid was reprecipitated from CH_2Cl_2/MeOH, filtered off, and washed with methanol to yield 571 mg (25.4%) of porphyrinogen.

To a solution of porphyrinogen (200 mg, 0.24 mmol) in 35 mL of CH_2Cl_2 was added 2,3-dichloro-5,6-dicyano-1,4-benzoquinone (DDQ)

(10) Shelnutt, J. A.; Medforth, C. J.; Berber, M. D.; Barigia, K. M.; Smith, K. M. *J. Am. Chem. Soc.* **1991**, *113*, 4077.
(11) Medforth, C. J.; Smith, K. M. *Tetrahedron Lett.* **1990**, *31*, 5583.
(12) (a) Takeda, J.; Ohya, T.; Sato, M. *Chem. Phys. Lett.* **1991**, *183*, *384*. (b) Ravikanth, M.; Reddy, D.; Chandrashekar, T. K. *J. Photochem. Photobiol. A: Chem.* **1993**, *72*, 61.
(13) Gentemann, S.; Medforth, C. J.; Forsyth, T. P.; Nurco, D. J.; Smith, K. M.; Fajer, J.; Holten, D. *J. Am. Chem. Soc.* **1994**, *116*, 7363.
(14) Levine, L. M. A.; Holten, D. *J. Phys. Chem.* **1988**, *92*, 714.
(15) (a) Rodriguez, J.; Kirmaier, C.; Holten, D. *Chem. Phys. Lett.* **1988**, *147*, 235. (b) Rodriguez, J.; Kirmaier, C.; Holten, D. *J. Am. Chem. Soc.* **1988**, *111*, 6100.
(16) Vitols, S. E.; Kumble, R.; Blackwood, M. E., Jr.; Roman, J. S.; Spiro, T. G. *J. Phys. Chem.* **1996**, *100*, 4180.
(17) Ryan, D. E. Ph.D. Dissertation, Princeton University, 1991.
(18) Ramirez, F.; Dershowitz, S. *J. Org. Chem.* **1957**, *22*, 41.
(19) Cheng, D. O.; LeGoff, E. *Tetrahedron Lett.* **1977**, *12*, 1469.
(20) Chamberlin, K. S.; LeGoff, E. *Heterocycles* **1979**, *12*, 1567.

(216 mg, 0.96 mmol). The pink solution became dark green almost immediately, and the reaction mixture was heated to reflux under argon for 30 min. After concentration of the solution via reduced pressure, the residue was chromatographed on neutral alumina (activity III, 2.5 8 cm) using 2% MeOH in CH_2Cl_2 as eluant. The major green fraction was collected, while a small amount of insoluble purple material remained at the top of the column. This purple material was dissolved in a 0.4% KOH/ethanol solution, the mixture was filtered, and the filtrate was combined with the green fraction. After removal of solvents, the residue was dissolved in CH_2Cl_2 and methanol. Several drops of triethylamine were added, and the green solution turned dark orange-brown. The CH_2Cl_2 was removed under reduced pressure, and the remainder was chilled and filtered to yield shimmering blue crystals. The product was washed with a minimal amount of cold methanol and vacuum-dried to afford 153 mg (76% based on porphyrinogen) of $OETPP(H)_2$. Mp → 300 °C. λ_{max} (CH_2Cl_2), nm (log ϵ): 350 (4.36), 456 (5.21), 556 (4.14), 602 (4.06), 632 (sh) (3.97), 708 (3.92). ^{1}H NMR ($CDCl_3$): δ 8.31 (m, 8H, *o*-H) 7.68 (m 12H, *m*,*p*-H), 2.51 (m (br), 8H, CH), 1.94 (m (br), 8H, CH_2), 0.44 (t (br), 24H, CH_3), −2.0 (s (br), 2H, NH). FTIR (KBr): 1596, 1442, 1371, 1113, 1054, 1016, 755 (vs), 736, 702 (vs) cm^{-1}. FAB-MS gave a parent ion peak at *m*/*z* 840. The precise mass pattern matched very well with a computer-simulated spectrum of $OETPP(H)_2$ ($C_{60}H_{62}N_4$). The wavelengths of the electronic absorption bands differ somewhat from those cited in ref 1a, and they did not change upon addition of triethylamine. However, when trifluoroacetic acid was added to a solution of the free base, the color changed from pale to bright green along with the observed absorption maxima shifts (λ_{max} = 400, 468, 636, 652, 690 nm). We therefore believe that the free base rather than the dication is prepared with our protocol.

Ru^{II}OETPP(CO). A 25 mL three-neck flask was charged with $OETPP(H)_2$ (20 mg, 2.38 × 10^{-5} mol), $Ru_3(CO)_{12}$ (77 mg, 1.20 × 10^{-4}), and 10 mL of Decalin. The mixture was refluxed under argon for 20 h and the reaction monitored by visible spectroscopy. Upon cooling, the entire mixture was chromatographed on neutral alumina. After being eluted successively with hexanes, benzene, and dichloromethane, the olive-brown fraction was collected using 5% MeOH in CH_2Cl_2. This collected band was chromatographed again on alumina using C_6H_6, 50:50 C_6H_6/CH_2Cl_2 ,and 100% CH_2Cl_2. The broad olive-colored band was eluted and the solvent removed under reduced pressure. Attempts to further purify the product by TLC on silica (CH_2Cl_2) resulted in partial decomposition. Therefore, the isolated brown Ru^{II}OETPP(CO) was vacuum-dried and stored in darkness at −15 °C. λ_{max} (CH_2Cl_2): 338, 418, 448 (sh), 558, 596 nm. ^{1}H NMR ($CDCl_3$): δ 8.28 (d, 8H, J = 6.7 Hz, *o*-H), 7.66 (m 12H, *m*,*p*-H), 2.19 (m (br), 16H, CH_2), 0.46 (t (24H), J = 7.4, 6.7 Hz, CH_3). FTIR (KBr): 2969, 2929, 2871, 1931 (vs), 1443, 1173, 1019, 760, 744, 702 cm^{-1}. FAB-MS gave the expected base peak at *m*/*z* 968 amu (M + 2) for $C_{61}H_{60}N_4ORu$.

Ru^{II}OETPP(Py)$_2$. A solution of 10 mg of RuOETPP(CO) in 5 mL of distilled pyridine was prepared under an inert atmosphere of nitrogen. The olive-brown solution was gently heated to 30 °C while being purged with argon. The solution was then irradiated by an Xe lamp for 30 min while being flushed with argon and monitored with visible spectroscopy. The pyridine was removed under reduced pressure, and the residue was eluted through a neutral alumina column with pure CH_2Cl_2. The major brownish-olive fraction was collected, dried under vacuum, and stored in darkness at −15 °C. λ_{max} (pyridine): 432, 510, 540 nm.

Transient Absorption (TA) and Time-Resolved Resonance Raman (TR^3) Spectroscopy. The nanosecond time-resolved absorption and RR apparatus have been described previously.[16] The ground state RR spectra of the Ru^{II}OETPP complexes were recorded with a triple polychromator equipped with an intensified diode array detector (Princeton Instruments) utilizing a 135° backscattering geometry.

For the transient spectroscopy, sample solutions were prepared under an inert atmosphere of nitrogen in a glovebox (Vacuum Atmospheres D1-001-SD equipped with an He-493 Dri-Train) and diluted to a final concentration of ∼1.5 mM (transient absorption) or ∼1 mM (transient Raman) by assuming an extinction coefficient of 300 000 cm^{-1} M^{-1} at the Soret band maximum.[21] Solutions were placed in a 1 cm (TA) or 1 mm (TR^3) path length cuvette modified with a Teflon stopcock attached to the stem to prevent sample contamination with oxygen. Sample integrity was monitored by comparison of probe-only spectra taken before and after each time point as well as by comparison of bulk absorption spectra taken before and after each experiment. TA spectra were calibrated using HeNe, Ar^+, and Kr^+ emission lines. The TR^3 difference spectra were obtained by subtracting the "probe-only" spectra from the "pump + probe" spectra. The intensity ratio for the subtraction procedure was adjusted to avoid negative peaks.

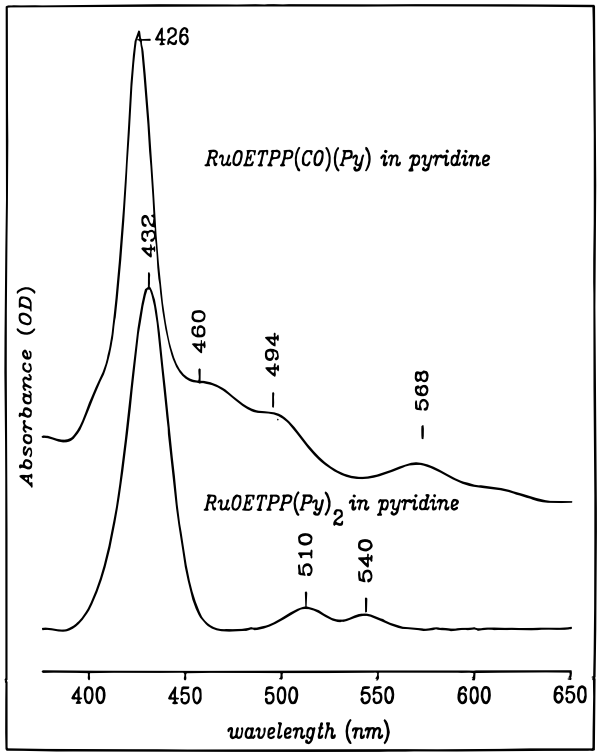

Figure 2. Absorption spectra for the indicated complexes of Ru^{II}OETPP.

Table 1. Electronic Absorption Maxima (nm) for Various Ru^{II}(porphyrin)(L′)(L) Complexes

complex	solvent	Soret [B(0,0)]	β [Q(1,0)]	α [Q(0,0)]	other
NiOETPP[a]	CH_2Cl_2	434	552	588	*d*
RuOETPP(CO)	CH_2Cl_2	418	558	*d*	448 (sh), 596
RuOETPP(CO)Py	pyridine	426	568	*d*	460 (sh), 494
$RuOETPP(Py)_2$	pyridine	432	510	540	*d*
RuOEP(CO)(Py)[b]	CH_2Cl_2	396	518	549	*d*
$RuOEP(Py)_2$[b]	benzene	395	495	521	450, 514
RuTPP(CO)(Py)[c]	pyridine	412	531	*d*	*d*
$RuTPP(Py)_2$[c]	pyridine	412	506	*d*	426 (sh)

[a] Data obtained from ref 3. [b] Data obtained from ref 22. [c] Data obtained from ref 14. [d] Unobserved.

Results

Ground State Optical Absorption Spectra. Absorption spectra of the Ru^{II}OETPP species (Figure 2 and Table 1) reveal red-shifted $\pi-\pi^*$ electronic transitions, as has been observed for other OETPP complexes.[1a,3] Both the B and Q bands are found at longer wavelengths than those for corresponding OEP and TPP analogs. The red shift in the optical spectra of ruffled porphyrins is attributed to a decrease in the energy separating the highest occupied molecular π orbitals from the lowest unoccupied π^* molecular orbitals. The decrease in separation

(21) Smith, K. M. *Porphyrins and Metalloporphyrins*; Elsevier: New York, 1975.

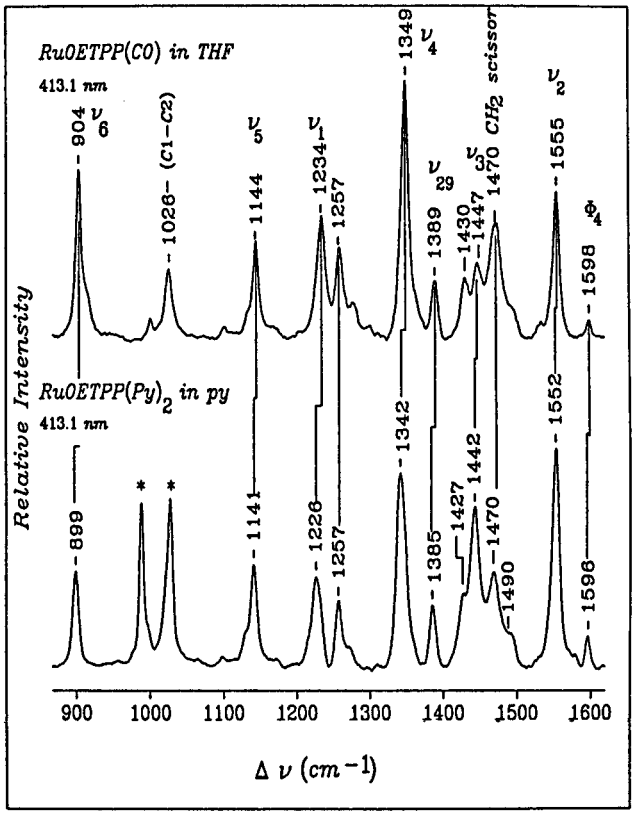

Figure 3. Resonance Raman spectra of the indicated complexes, with B-band excitation (413.1 nm). Asterisks mark pyridine solvent bands.

is principally caused by the destabilization of the HOMOs by the out-of-plane distortions, which raises their energies. In contrast, the energies of the degenerate LUMOs remain unchanged.[1a,d,3]

Relative to those of other metals, however, the Ru(II) B and Q bands are blue-shifted. This well-known hypsochromic effect of Ru(II)[14,22] is attributed to the strong Ru(II)→porphyrin back-bonding, which raises the energy of the porphyrin e_g* orbitals via interaction with the Ru(II) d_π orbitals. The effect is especially pronounced when the axial ligands are pyridine but is diminished when one or both pyridines are replaced by CO. The Q-band red shift for Ru^{II}OETPP(CO)(Py) relative to Ru^{II}OETPP$(Py)_2$, also seen for the OEP and TPP analogs (Table 1), is due to the competition of the CO π* orbitals with the porphyrin e_g* orbitals for the Ru(II) d_π electrons. This competition diminishes the $d_\pi-e_g$* interaction and lowers the e_g* orbital energy. For the OEP and TPP analogs, the lowered HOMO/LUMO gap results in a red shift of the Q bands, but the B band is unaltered (Table 1). For OETPP, the B band actually appears to blue shift, but this effect may result from overlap with another, unidentified electronic transition, since the 432 nm B band of Ru^{II}OETPP$(Py)_2$ is quite broad, while Ru^{II}OETPP(CO)(Py) has a 460 nm shoulder on its (narrow) 426 nm B band.

This unidentified transition is not a Ru → pyridine charge-transfer transition, since the RR spectra (see below) show no enhancement of bound pyridine modes. Such modes are seen in the spectrum of Ru^{II}OEP$(Py)_2$ when the excitation is in resonance with absorption bands appearing between the B and Q bands, which are assigned to Ru → pyridine charge-transfer

(22) Antipas, A.; Buchler, J. W.; Gouterman, M.; Smith, P. D. *J. Am. Chem. Soc.* **1978**, *100*, 3015.

Table 2. Resonance Raman Band Frequencies (cm^{-1})

mode[a]	Ru-OETPP(CO)	Ru-OETPP$(Py)_2$	$\Delta\nu$[b]	$\Delta\nu$(TPP)[c]	$\Delta\nu$(OEP)[c]
ϕ_4 ν(CC)	1598	1596	−2	0	*d*
ν_2 $\nu(C_\beta C_\beta)$	1555	1552	−3	0	+4
$-CH_2$ scissors	1470	1470	0	*d*	*d*
ν_3 $\nu(C_\alpha C_m)$	1447	1442	−5	−4	−4
ν_{29} $\nu(C_\alpha C_m)$	1389	1385	−4	*d*	−3
ν4 $\nu(C_\alpha N)_{sym}$	1349	1342	−7	−5	−14
$-CH_2$ twist	1257	1257	0	*d*	0
ν_1 $\nu(C_m C_{Ph})$	1234	1226	−8	−5	*d*
ν_5 $\nu(C_\beta C_1)$	1144	1141	−3	*d*	*d*
ν_6 pyr breathing	904	899	−5	*d*	*d*

[a] Assignments from ref 3. [b] Frequency differences between the CO adduct and the $(Py)_2$ adduct. [c] $(Py)_2$ minus CO frequency differences for Ru^{II}TPP and Ru^{II}OEP.[26] [d] Unobserved or uncertain.

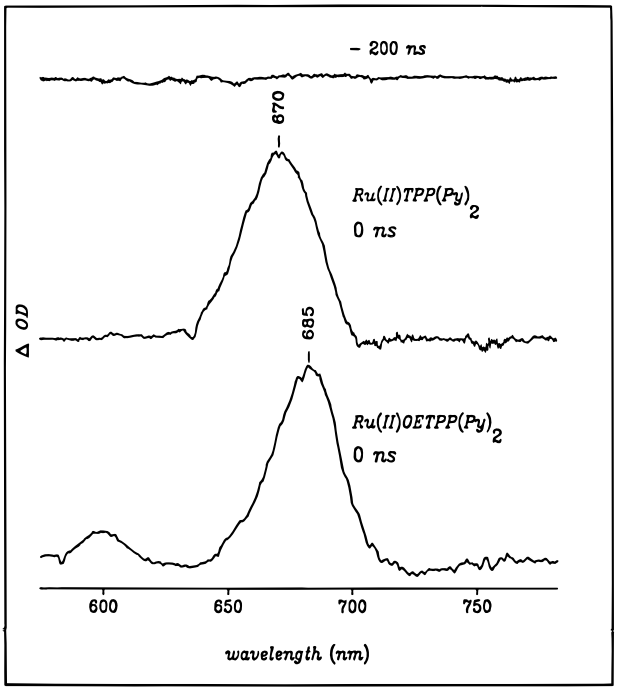

Figure 4. Photoinduced absorption spectra for the indicated complexes with temporal overlap of pump (416 nm) and probe (broad band) pulses (0 ns). The top trace, with the probe preceding the pump (−200 ns), is the background.

transitions.[23] In this respect, Ru^{II}OETPP$(Py)_2$ resembles Ru^{II}TPP$(Py)_2$ in showing no evidence for Ru → pyridine charge-transfer transitions.[16]

Ground State Resonance Raman Spectra. Further evidence of π-back-bonding effects is seen in the RR spectra of Ru^{II}OETPP(CO)(Py) and Ru^{II}OETPP$(Py)_2$ (Figure 3). The bands are assigned with reference to NiOETPP,[3] and it can be seen that the frequencies of several skeletal modes (ν_1, ν_3, ν_4, ν_6, ν_{29}) downshift significantly when CO is replaced by a pyridine ligand. This effect also occurs in OEP and TPP adducts[26] (Table 2) and is attributed to increased back-donation to the porphyrin e_g* orbitals when competition from the CO π* orbitals is eliminated. By populating the antibonding e_g* orbital, the enhanced back-donation weakens bonds in the

(23) (a) Schick, G. A.; Bocian, D. F. *J. Am. Chem. Soc.* **1984**, *106*, 1682. (b) Barrow, W. L. Resonance Raman Studies of Charge-Transfer Compounds. Dissertation Georgia Institute of Technology, 1982.
(24) Choi, S.; Spiro, T. G.; Langry, K. C.; Smith, K. M.; Budd, L. D.; LaMar, G. N. *J. Am. Chem. Soc.* **1982**, *104*, 4345.
(25) Parthasarathi, N.; Hansen, C.; Yamaguchi, S.; Spiro, T. G. *J. Am. Chem. Soc.* **1987**, *105*, 3865.
(26) Kim, D.; Su, O. Y.; Spiro, T. G. *Inorg. Chem.* **1986**, *25*, 3993.

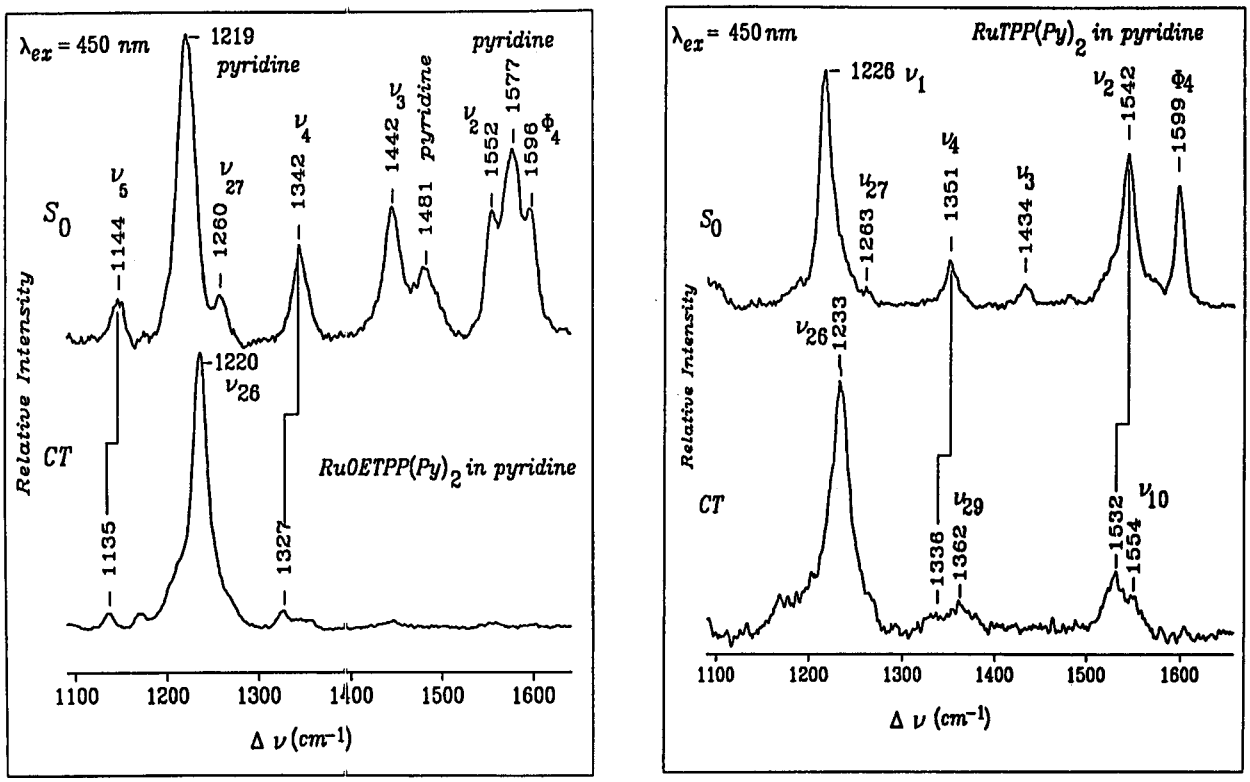

Figure 5. RR spectra of the excited states of RuOETPP(Py)$_2$ (left, bottom) and RuTPP(Py)$_2$ (right, bottom) obtained by subtracting the ground state spectra (450 nm pulsed excitation, top) from the spectra induced by pumping at 416 nm and probing at 450 nm, with temporal overlap of the pulses. The RuOEPTPP(Py)$_2$ ground state spectrum contains strong pyridine solvent bands (1219, 1481, and 1577 cm^{-1}) because of sample dilution (necessitated by degradation reactions encountered at higher concentrations).

porphyrin ring, leading to downshifts of skeletal modes. Although the modes differ significantly in frequency and composition among OEP, TPP, and OETPP,[3] the pattern of frequency shifts for the Ru(II) adducts is similar (Table 2). As expected, modes associated with internal vibrations of the substituents shift very little (e.g., the ϕ_4 phenyl mode and the CH_2 scissors mode in the OETPP spectra—Figure 3). Excitation of Ru^{II}OETPP(CO)(Py) at other wavelengths (457.9 and 472.7 nm) produced spectra with somewhat altered intensity patterns, but there was no evidence of bound-pyridine modes, as there is for Ru^{II}OEP(Py)$_2$.[23]

Transient Absorption Spectra. When Ru^{II}OETPP(Py)$_2$ is photoexcited, an induced absorption is observed at 685 nm (Figure 4) in a region characteristic of charge-transfer states.[15b] A similar absorption is seen for Ru^{II}TPP(Py)$_2$ but with a maximum at 670 nm. The lowest excited state of Ru^{II}TPP(Py)$_2$ is known to be charge transfer in character,[15b,16] and a similar excited state is inferred for Ru^{II}OETPP(Py)$_2$. The red shift in its absorption relative to that of Ru^{II}TPP(Py)$_2$ is consistent with the red-shifts of the $\pi-\pi^*$ absorptions in the ground state.

TR^3 Spectra. Figure 5 compares ground and excited state RR spectra for Ru^{II}OETPP(Py)$_2$ (left) and Ru^{II}TPP(Py)$_2$ (right). The ground state spectra were obtained with 450 nm excitation with a 10 Hz, 7 ns H_2-Raman-shifted pulsed Nd:YAG laser, while the excited state spectra were obtained by subtracting the ground state spectra from the photoinduced spectra produced by the same probe pulses when temporally overlapped with 416 nm pump pulses. (The appearance of strong peaks from the pyridine solvent in the ground state spectrum of Ru^{II}OETPP(Py)$_2$ but not Ru^{II}TPP(Py)$_2$ is due to a lower sample concentration for the former. The concentration of the RuOETPP(Py)$_2$ sample had to be lowered in order to prevent degradation of the sample from photochemistry occurring at higher concentrations.)

The resemblance of the two excited state spectra is apparent. Both are dominated by a strong band near 1200 cm^{-1}, which is assigned[16] to the skeletal mode ν_{26}. They both show a 15 cm^{-1} downshift of the ν_4 mode and enhancement of a neighboring band assigned to ν_{29}. The enhancement of the non-totally symmetric modes ν_{29}, and especially ν_{26}, is attributed to a Jahn–Teller effect in the excited state, which splits the degeneracy of the e_g* acceptor orbitals and renders the vibrational modes totally symmetric. In the Ru^{II}TPP(Py)$_2$ excited state, enhancement is also seen for ν_2, downshifted from its ground state position, and another non-totally symmetric mode, identified as either ν_{10} or ν_{11}. For Ru^{II}OETPP(Py)$_2$, these bands are too weak to be identified reliably. Nevertheless, the similarity of the two spectra, and their relationship to porphyrin anion RR spectra,[16] makes it apparent that they arise from the same kind of excited state, namely a Ru(II) → porphyrin charge transfer state. The downshifts in ν_4 and ν_2 reflect weakening of porphyrin bonds when an electron is promoted to the e_g* orbitals.

Significantly, no bound pyridine modes are detected in the excited state spectrum of Ru^{II}OETPP(Py)$_2$, in contrast to that of Ru^{II}OEP(Py)$_2$. The charge transfer state involves acceptor orbitals on the porphyrin, not on the pyridine.

Discussion

Strong back-bonding from Ru(II) to the porphyrin e_g* LUMO is evidenced by depressed porphyrin skeletal mode frequencies in the RR spectrum of Ru(II) porphyrins and by the short-lived $d\pi \rightarrow \pi^*$ character of the lowest electronic excited state.[16] Back-bonding to the porphyrin is weakened when CO is an axial ligand, because the CO π^* orbitals compete effectively for the Ru(II) $d\pi$ electrons; as a result, the skeletal mode frequency downshifts are relieved and the $d\pi \rightarrow \pi^*$ excited state is raised in energy above the lowest $\pi-\pi^*$ state. It is evident that these

consequences of back-bonding are also seen for Ru^{II}OETPP-$(Py)_2$: the skeletal mode frequencies are depressed relative to those of Ru^{II}OETPP(CO), and the lowest excited state is $d\pi \rightarrow \pi^*$ in character. This was not a foregone conclusion, since porphyrin ruffling induced by the substituent crowding might have been expected to diminish back-bonding because of orbital misalignment. The out-of-plane distortion is probably less pronounced in $Ru^{II}OETPP(Py)_2$ than in NiOETPP or CuOETPP, since the distortion increases with decreasing metal−N (pyrrole) distance, and Ru(II) is larger than Ni(II) and Cu(II); for $RuOEP(CO)(H_2O)$, this distance is 2.051 Å,[27] compared to 1.998 Å for CuOEP[28] and 1.958[29] or 1.929 Å[30] for planar or ruffled allotropes of NiOEP. The out-of-plane distortion in OETPP remains substantial even for large metal ions, e.g. in ZnOETPP-(MeOH) (Zn−N = 2.063 Å.)[31] However, it is possible that $Ru^{II}OETPP(Py)_2$ resists distortion, even at the expense of steric crowding, in order to preserve the back-bonding. Its crystal structure would therefore be of considerable interest.

Another point of interest is that the $Ru^{II}OETPP(Py)_2$ TR^3 spectrum allows us to conclude that the direction of excited state electron transfer is dominated by the phenyl rather than by the ethyl substituents. We recently found that while the electron is transferred from Ru(II) to the porphyrin in the lowest excited state of $Ru^{II}TPP(Py)_2$, it is transferred instead to the pyridine ligands in $Ru^{II}OEP(Py)_2$.[16] The evidence for this conclusion was that the TR^3 spectrum of the ligands in $Ru^{II}OEP(Py)_2$ showed upshifted porphyrin skeletal modes, as would be expected for a Ru(III) porphyrin, together with additional bands which were identified by isotope labeling as pyridine anion modes. Evidently, the ethyl substituents, which are electron donating, raise the porphyrin e_g* orbitals above the lowest pyridine π* orbital in $Ru^{II}OEP(Py)_2$. This inference is supported by the detection of relatively low-energy Ru(II) → Py charge-transfer transitions that selectively enhance pyridine RR bands of $Ru^{II}OEP(Py)_2$.[23] Such transitions were not found in $Ru^{II}TPP(Py)_2$;[16] the phenyl substituents are electron withdrawing and stabilize the e_g* orbitals. Nor are Ru(II) → Py charge-transfer transitions present in $Ru^{II}OETPP(Py)_2$, whose TR^3 spectrum likewise resembles that of $Ru^{II}TPP(Py)_2$. Both TR^3 spectra are consistent with a Ru(III) porphyrin anion formulation and show no evidence for pyridine anion modes. Thus, when phenyl and ethyl substituents are both present, the phenyl influence dominates the ethyl influence. This result is consistent with the e_g* orbital structure, in which the coefficients are larger on the C_m atoms, where the phenyl substituents are attached, than on the C_β atoms, where the ethyl substituents are attached.[32]

Acknowledgment. This work was supported by NIH Grant GM 33576.

IC960773H

(27) Kadish, K. M.; Hu, Y.; Mu, X. H. *J. Heterocycl. Chem.* **1991**, *28*, 1821.
(28) Pak, R.; Scheidt, W. R. *Acta Crystallogr.* **1991**, *C47*, 431.
(29) Cullen, D. L.; Meyer, E. F. *J. Am. Chem. Soc.* **1974**, *96*, 2095.
(30) Meyer, E. F.; *Acta Crystallogr.* **1972**, *B28*, 2162.
(31) Barkigia, K. M.; Berber, M. D.; Fajer, J.; Medforth, C. J.; Renner, M. W.; Smith, K. M. *J. Am. Chem. Soc.* **1990**, *112*, 8851.
(32) Sekino, H.; Kobayashi, H. *J. Chem. Phys.* **1987**, *86*, 5045.